JOURNAL OF SOLID STATE CHEMISTRY 89, 299–307 (1990)

Synthesis and Characterization of $LaTi_{1-x}Cu_xO_3$ Compounds

M. L. ROJAS AND J. L. G. FIERRO*

Instituto de Catálisis y Petroleoquímica, C.S.I.C., Serrano 119, 28006 Madrid, Spain

Received March 5, 1990; in revised form July 18, 1990

Substituted perovskites of the type $LaTi_{1-x}Cu_xO_3$ have been synthetized and characterized by means of X-ray diffraction, temperature-programmed reduction, and X-ray photoelectron spectroscopy. For the unsubstituted ($x = 0$) and substituted $x = 0.2$ compounds, the only phases present were $La_2O_3 \cdot 2TiO_2$ and $La_2O_3 \cdot 3TiO_{1.9}$ in the former case, and these two mixed oxides together with CuO, La_2CuO_4, and $2La_2O_3 \cdot 3TiO_2$ in the latter. For higher substitutions in the range $0.3 \leq x \leq 0.8$, the perovskite structure was observed, while for $x = 1$ the only phases were CuO and La_2CuO_4. The TPR profile for $LaTiO_3$ showed a very small weight loss, which indicates a high stability of the oxide. Samples with substitutions $0.2 \leq x \leq 0.8$ revealed two reduction steps of Cu^{2+} to Cu^0: first at a low temperature, and in a very narrow temperature window, due to the separate CuO phase, and second at a higher temperature, extending in a very large temperature range, due to the perovskite phase. Finally, in the fully substituted ($x = 1.0$) sample reduction of CuO and La_2CuO_4 phases were clearly differentiated. In addition, XPS data revealed that reduction of $LaTi_{1-x}Cu_xO_3$ ($x = 0.2$ and 0.4) samples yielded maximum copper exposure at temperatures ca. 623 K while copper particles underwent important sintering at higher temperatures of reduction.

Introduction

Perovskite-type oxides, of the general formula ABO_3, have long been studied because they exhibit technologically important physical properties (*1–4*). The diversity of properties of the perovskites is derived on one hand from the large variety of A and B ions which fit into the crystal structure, and on the other hand from the variation in the valence states of the transition metal ions which can be controlled by the proper choice of the A ions. Substituted perovskites of the type $A_{1-x}A'BO_3$, $AB_{1-y}B'_yO_3$ or even $A_{1-x}A'_xB_{1-y}B'_yO_3$ (where A' and B' are ions substituted into the A site and B sites, respectively) add to the capability of tailoring specific properties. This accounts for the great variety of reactions in which the perovskites have been used as catalysts (see, e.g., (*5*) and references therein). Moreover, the A ions are, in general, catalytically inactive, and the active transition metal ions at the B position are placed at sufficiently large distances from each other (ca. 0.4 nm) so that a gas molecule can interact with a single site (*6*).

As special interest has recently been focused on the production of oxygenated compounds from syngas ($CO + H_2$), it was postulated that some reducible perovskites could be used as model catalysts for this reaction. Unsubstituted $LaRhO_3$ (*7–10*) and substituted $LaM_{0.5}Cu_{0.5}O_3$ (M = Mn, Ti) (*11, 12*) have hence been used for such a purpose. Broussard and Wade (*11*) reported

* To whom correspondence should be addressed.

0022-4596/90 $3.00

that the substituted $LaM_{0.5}Cu_{0.5}O_3$ ($x = 0.5$) oxides exhibited high methanol selectivity, while the unsubstituted $LaMO_3$ ($x = 0$) perovskites were inactive in the formation of oxygenates. From data obtained with other perovskites these authors also concluded that the catalytic centers responsible for the reaction are the higher valence surface cations in the *B* position ($B^{\delta+}$, $\delta > 0$). Likewise, in very recent work Brown *et al.* (*12*) studied the CO hydrogenation over $LaMn_{1-x}Cu_xO_3$ ($x = 0.0$–1.0) perovskite series synthetized by Rojas *et al.* (*13*) and found that the $LaMnO_3$ ($x = 0$) perovskite was weakly active for CO hydrogenation, and produced only hydrocarbons, whereas the other substituted perovskites ($0.2 < x < 0.8$) were much more active and displayed high selectivity for methanol and higher alcohols. These authors proposed that hydrocarbon synthesis occurs at Cu° sites, but that Cu° and Cu^+ sites are required for the formation of alcohols. It appears, therefore, that $Cu^{\delta+}$ ($\delta > 0$) sites should play an important role in the syngas conversion to oxygenates.

With a few exceptions (*8, 10, 13*), the studies carried out so far provide little information on either bulk or surface properties of these materials. In this study, the synthesis and some bulk and surface properties of the family of $LaTi_{1-x}Cu_xO_3$ ($x = 0.0$–1.0) compounds are reported. For this purpose, temperature-programmed reduction (TPR), X-ray diffraction (XRD), and X-ray photoelectron spectroscopy (XPS) techniques have been used.

Experimental

Materials

The substituted $LaTi_{1-x}Cu_xO_{3+\delta}$ ($0 \leq x \leq 1$) compounds were prepared by amorphous citrate decomposition as described earlier (*14*). In the synthesis, $La(NO_3)_3 \cdot 6H_2O$, citric acid, p.a. from Merck, Cu $(CH_3\text{–}COO)_2 \cdot H_2O$ from Carlo Erba, and Ti *n*-$(BuO)_4$ (98% ex-Ti) from Aldrich-Chemie were used. Other compounds employed either in TPR or in XPS were as follows: TiO_2 (87% anatase) from Degussa; CuO, analytical grade from Mallinckrodt; and La_2O_3 was obtained by thermal decomposition of $La(NO_3)_3 \cdot 6H_2O$, at 673 K in air, p.a. from Merck.

Methods

Temperature-programmed reduction measurements were conducted on a Cahn 2100 RG microbalance, operating with 10 μg accuracy. The 20-mg sample was first heated in a He flow at a rate of 4 K min^{-1} up to 673 K and then it was cooled down to 373 K under He flow. Then the temperature was increased at the same rate while passing H_2 through the sample, as above, until 1023 K was reached. The observed weight losses were taken as a measure of the extent of the reduction.

X-ray diffraction patterns were obtained with a Philips PW1716/30 diffractometer using nickel-filtered Cu$K\alpha$ radiation. Care was taken with the H_2-reduced materials. To avoid excessive oxidation upon air exposure, reduced samples were passivated in 1% (v/v) air: He for 12 hr at ambient temperature. The X-ray diffraction patterns were recorded over the range of 2Θ angles ranging from 5–70° and the *d*-spacings were compared with the ASTM powder files to confirm sample identity. The BET surface areas were calculated from the nitrogen adsorption isotherms at 77 K using a value of 0.164 nm^2 for the cross-section of the N_2 molecule.

X-ray photoelectron spectra were recorded on a Leybold LHS 10 spectrometer with a hemispherical electron energy analyzer and Mg$K\alpha$ (1253.6 eV) X-ray radiation source. The samples were pressed into small Inox holders and mounted on a standard sample rod, placed in an introduction chamber, and pumped at ca. 10^{-5} Torr (1 Torr = 133.33 Nm^{-2}) before they were moved into the turbopumped analysis chamber. The residual pressure during data acquisition was

maintained below 7×10^{-9} Torr. Either 20- or 50-eV energy regions of the photoelectrons of interest were acquired at 20-eV spectrometer pass energy, chosen as a compromise to enable acceptable energy resolution to be obtained within reasonable data collection times. Each spectral region was signal averaged for a number of scans to obtain good signal-to-noise ratios. Accurate binding energies (BE) were determined by charge referencing with the C1*s* line at 284.6 eV.

Results and Discussion

X-Ray Diffraction

X-ray diffraction patterns of the as-prepared samples with nominal composition $LaTi_{1-x}Cu_xO_3$ ($0 < x < 1$) were obtained. The representative XRD patterns are summarized in Fig. 1. For the X-ray pattern of the unsubstituted ($x = 0$) compound, there appear lines which can be indexed as belonging to $La_2O_3 \cdot 2TiO_2$ and $La_2O_3 \cdot 2TiO_2$ and $La_2O_3 \cdot 3TiO_{1.9}$. For substitution of Ti by Cu up to $x = 0.2$ the dominant peaks in the XRD pattern correspond to the same mixed oxides, but other weak peaks indexed as La_2CuO_4, CuO, and $2La_2O_3 \cdot 3TiO_2$ oxide lines are observed. Substitution of Ti by Cu in the range $0.3 \leq x \leq 0.8$ gives rise to the appearance of the perovskite structure. Although the XRD pattern of the perovskite is very clean, other very weak reflections indexed as CuO can be observed in the background. For substitution of Ti by Cu ($x = 1.0$) the only phases present are La_2CuO_4 and CuO. This latter result is a little surprising when compared with literature findings. For instance, the synthesis of pure $LaCuO_3$ perovskite has been reported by Demazeau *et al.* (*15*), and mixed $LaCuO_3$ perovskite and La_2CuO_4 and CuO phases have been found by Gallagher *et al.* (*16*) and Vogel *et al.* (*17*) in the preparation of copper-rich $LaMn_{1-x}Cu_xO_3$ ($0.7 \leq x \leq 1.0$) compounds. In light of these results we can infer that our preparations with nominal composition $LaCuO_{2.5}$ (or $La_2Cu_2O_5$) is not stable under the experimental conditions.

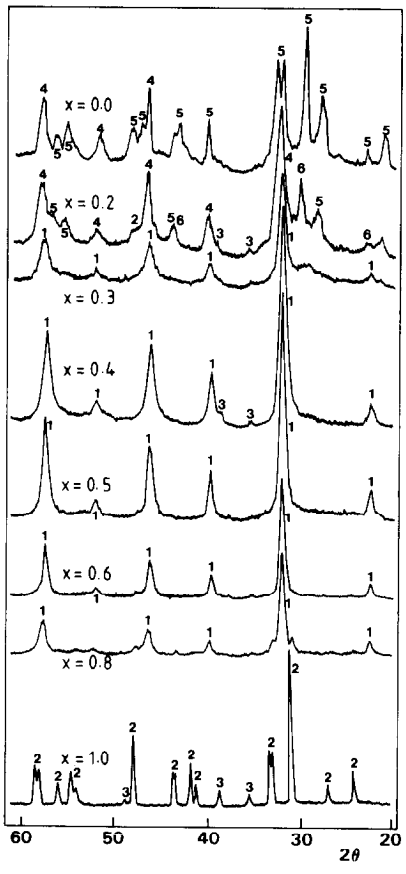

FIG. 1. X-ray diffraction patterns (Cu$K\alpha$ radiation) of oxidized $LaTi_{1-x}Cu_xO_3$ samples. Crystalline phases are as follows: 1, perovskite; 2, La_2CuO_4; 3, CuO; 4, $La_2O_3 \cdot 3TiO_{1.9}$; 5, $La_2O_3 \cdot 2TiO_2$; 6, $2La_2O_3 \cdot 3TiO_2$.

As defined by Goldschmidt (*18*),

$$t = \frac{r_{La} + r_0}{\sqrt{2}\,(r_{Cu} + r_0)} \qquad (1)$$

(r_{La}, r_0, and r_{Cu} are the ionic radii of La^{3+}, O^{2-}, and Cu^{2+}, respectively), the $La_2Cu_2O_5$ oxide has a rather low tolerance factor of 0.86, which explains its instability (*13*). Lanthanides of the type $La_2M_2O_5$ are known for a variety of M^{2+} cations. Crespin *et al.* (*19*)

reported evidence of formation of $La_2Ni_2O_5$ upon H_2-reduction of a $LaNiO_3$ perovskite at 585 K, which was transformed to La_2NiO_4 and NiO upon heating in He at 1273 K. In addition, Nakamura *et al.* (*20*) found La_2NiO_4 and La_2CoO_4 phases upon heating $LaNiO_3$ and $LaCoO_3$ oxides at 1273 K in a reducing atmosphere. In agreement with these findings, Fierro *et al.* (*21*) have also reported the formation of La_2NiO_4 after heating at 1073 K in He a $LaNiO_{2.5}$ phase.

At the other composition extreme $x = 0$, the absence of $LaTiO_3$ perovskite indicates that such a structure is not obtained under the conditions of the synthesis. Many titanates of the general formula $MTiO_3$ (M = divalent cation and tetravalent titanium) have been synthetized at moderately high temperatures (*22–26*). However, as Ti^{3+} ions are present in $LaTiO_3$ the stabilization of these ions occurs at very high temperatures.

To identify the reduced species formed upon H_2-reduction at 950 K, XRD patterns of the reduced samples (Fig. 2) were obtained. As can be seen, the XRD pattern of the sample with nominal composition $LaTiO_3$ after reduction is similar to that of the as-prepared sample; only $La_2O_3 \cdot 2TiO_2$ and $La_2O_3 \cdot 3TiO_{1.9}$ phases are obtained. This means that reduction treatment does not alter the initial oxide. H_2-reduction of substituted $LaTi_{1-x}Cu_xO_3$ ($0.3 \leq x \leq 0.6$) samples gives rise to the products La_2O_3, $La_2O_3 \cdot 3TiO_{1.9}$ and Cu°. Only for samples with $x = 0.8$ and 1.0 were the $La(OH)_3$ and Cu° phases observed. In general, the intensities of diffraction lines are lower in reduced than in oxidized samples. This can be due to disappearance of the perovskite structure during reduction and formation of ill-defined crystalline La_2O_3 and $La_2O_3 \cdot 3TiO_{1.9}$ oxides at temperatures slightly lower than that used in synthesis. Note also that the bulk La_2O_3 is almost quantitatively transformed to $La(OH)_3$ after long exposure to moisture of the highly substituted ($x = 0.8$ and 1.0) samples. Particle sizes were calculated, by means of X-ray line broadening measurements and using the Debye–Scherrer equation (*27*). For this calculation the most intense Cu (111) peak in Fig. 2 was taken. The results obtained are summarized in Table I. By sample reduction with $x = 0.4$ at 970 K metallic copper of a particle size of 23.6 nm supported on a $La_2O_3 \cdot 3TiO_{1.9}$ matrix is obtained. Copper particle sizes decreased almost uniformly for reduced samples with higher substitutions ($x = 0.5$–0.8). This may be interpreted in terms of copper mobility,

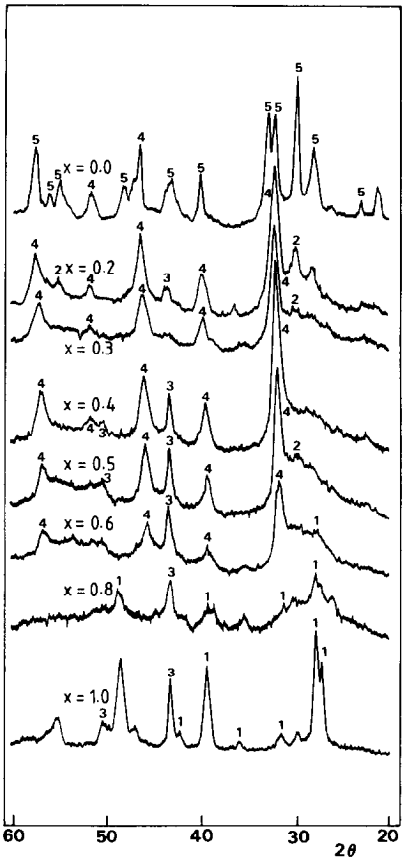

FIG. 2. X-ray diffraction patterns (Cu$K\alpha$ radiation) of $LaTi_{1-x}Cu_xO_3$ samples after H_2-reduction in TPR experiments. Crystalline phases are as follows: 1, $La(OH)_3$; 2, La_2O_3; 3, Cu; 4, $La_2O_3 \cdot 3TiO_{1.9}$; 5, $La_2O_3 \cdot 2TiO_2$.

TABLE I

CHARACTERISTICS OF THE REDUCED $LaTi_{1-x}Cu_xO_3$ PEROVSKITES

Substitution	Crystalline phases	d_{Cu} (nm)[a]	$TiO_{2-\lambda}$[b]
$x = 0.0$	La_2O_3, $La_2O_3 \cdot 3TiO_{1.9}$	—	—
0.2	La_2O_3, $La_2O_3 \cdot 3TiO_{1.9}$	—	—
0.3	La_2O_3, $La_2O_3 \cdot 3TiO_{1.9}$, Cu	—	$TiO_{1.98}$
0.4	$La_2O_3 \cdot 3TiO_{1.9}$, Cu	23.6	$TiO_{1.96}$
0.5	La_2O_3, $La_2O_3 \cdot 3TiO_{1.9}$, Cu	18.1	$TiO_{1.98}$
0.6	$La_2O_3 \cdot 3TiO_{1.9}$, Cu	14.8	$TiO_{1.97}$
0.8	$La(OH)_3$, Cu	12.6	$TiO_{2.00}$
1.0	La_2O_3, $La(OH)_3$, Cu	—	$TiO_{2.00}$
1.0	La_2O_3, $La(OH)_3$, Cu	—	—

[a] Only the most intense Cu(111) diffraction peak was considered.
[b] λ Is the nonstoichiometry degree.

which is greater in samples with lower substitutions, and hence it is easier to form larger Cu particles. It must be noted that reduction temperatures on the order of 0.60 Tamman's temperature of Cu strongly favor surface diffusion and further crystallization of copper atoms. These copper crystal sizes in the reduced samples do not hinder the oxidation of Cu and further reaction between the CuO, and La_2O_3 and $La_2O_3 \cdot 3TiO_{1.9}$ phases. This has been already confirmed for the reduced sample with $x = 0.4$, which upon air-oxidation up to 973 K fully reversed to the original perovskite phase.

Temperature-Programmed Reduction

TPR profiles of the $LaTi_{1-x}Cu_xO_3$ perovskites and the reference CuO oxide are given in Fig. 3. The overall reduction process of $LaTi_{1-x}Cu_xO_3$ oxides can be stated by the equation

$$2LaTi_{1-x}Cu_xO_3 + (4x - 1)H_2 \rightarrow La_2O_3 + 2xCu + 2(1 - x)TiO_2 + (4x - 1)H_2O.$$

Reduction of the unsubstituted $LaTiO_3$ compound led to a very small weight loss corresponding to ca. 0.4% at temperatures above 850 K. For substitutions $0.2 \leq x \leq 0.8$, the TPR profiles show, however, two different reduction steps. The first one at 440–570 K is very fast, and closely corresponds to the reduction of CuO to metallic Cu° (Fig. 3, dashed line), while the second one occurs at higher temperatures at a much slower rate, while the extent of the reduction of both steps increases, in general, with substitution. It is observed that H_2-reduction of copper ions placed in the perovskite structure is reached at substantially higher temperatures than in CuO, which indicates the increased stability of Cu^{2+} ions in the perovskite structure. In very close agreement with these results, Rojas *et al.* (*13*) have shown that in $LaMn_{1-x}Cu_xO_3$ perovskites, Mn^{4+} and Cu^{2+} ions are much more stable in a H_2 atmosphere than the respective MnO_2 and CuO oxides.

The fully substituted ($x = 1.0$) sample shows, however, two well-differentiated steps, the first one below 500 K and the second one above 600 K. As stated above,

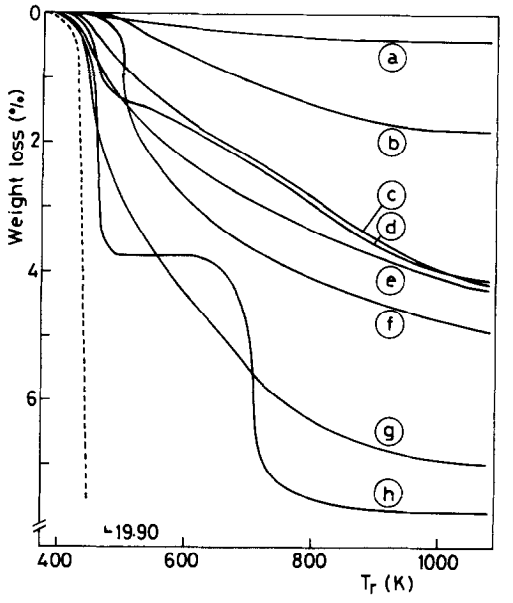

FIG. 3. Temperature-programmed reduction profiles of $LaTi_{1-x}Cu_xO_3$ samples with different substitution degree (x): a, 0.0; b, 0.2; c, 0.3; d, 0.4; e, 0.5; f, 0.6; g, 0.8; h, 1.0. Dashed line corresponds to bulk CuO reference.

the low temperature TPR peak is due to CuO reduction, while the high temperature TPR peak is due to the reduction of the more stable La_2CuO_4 oxide. This assignment is confirmed not only by the XRD diagram (Fig. 2), but also by the approximately equal weight losses in both high and low temperature TPR steps, which implies the distribution of copper over both phases, viz. CuO and La_2CuO_4. Therefore, the reduction process for the fully substituted ($x = 1.0$) sample can then be formulated according to the equation

$$CuO + La_2CuO_4 + 2H_2 \rightarrow 2Cu + La_2O_3 + 2H_2O.$$

Further insight on the nonstoichiometry of the resulting $TiO_{2-\lambda}$ oxide, formed upon H_2-reduction of the $LaTi_{1-x}Cu_xO_3$ perovskites, could be gained by comparing the experimental weight changes and the theoretical ones, assuming reduction of Cu^{2+} to Cu° and oxidation of Ti^{3+} to Ti^{4+}. The values of the nonstoichiometry factor (λ) are summarized in Table I. A very small deviation from the stoichiometry is found only in the substitution range $0.3 \leq x \leq 0.6$. However, these results contrast with the major crystalline titanium oxide ($TiO_{1.90}$) phase revealed by XRD. It must be noted that the molecular water, the product of H_2-reduction, reacts at once with La_2O_3 to form a very stable LaO(OH) phase (*5, 13, 28, 29*) instantly or even $La(OH)_3$ after long exposure to moisture (Table I). The small weight increase which also accompanies the reduction of perovskites is the result of two concomitant processes, viz. oxidation of Ti^{3+} and formation of LaO(OH) by the water produced during the reduction. Therefore, considering the above interpretation, values derived from TPR measurements can only be taken as an estimate of the nonstoichiometry of the titanium oxide.

X-Ray Photoelectron Spectroscopy

XP spectra of O1*s*, La4*d*, Ti2*p* and Cu2*p* core levels were recorded for $LaTi_{1-x}Cu_xO_3$ compounds subjected to outgassing under high vacuum and to reduction in H_2 at 473–723 K. Representative O1*s*, La4*d* and Cu2*p* spectra of $LaTi_{0.6}Cu_{0.4}O_3$ perovskite are given in Figs. 4, 5 and 6, respectively, and the corresponding BE values are summarized in Table II. The O1*s* spectra (Fig. 4) show the maximum at 528.9–529.9 eV and the line profile as depending on the pretreatments. The outgassed sample presents a rather symmetric O1*s* peak while the H_2-reduced ones show a long tail extending in

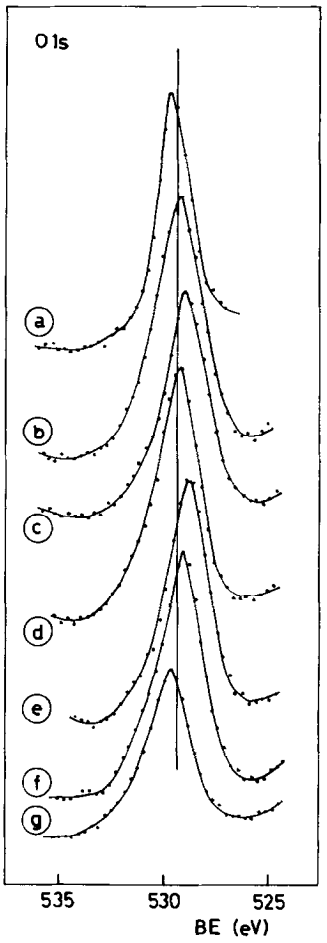

FIG. 4. O1*s* core level spectra of $LaTi_{0.6}Cu_{0.4}O_3$ samples subjected to (a), outgassing at 723 K, and to reduction in hydrogen at (b) 473 K, (c) 523 K, (d) 573 K, (e) 623 K, (f) 673 K, (g) 723 K.

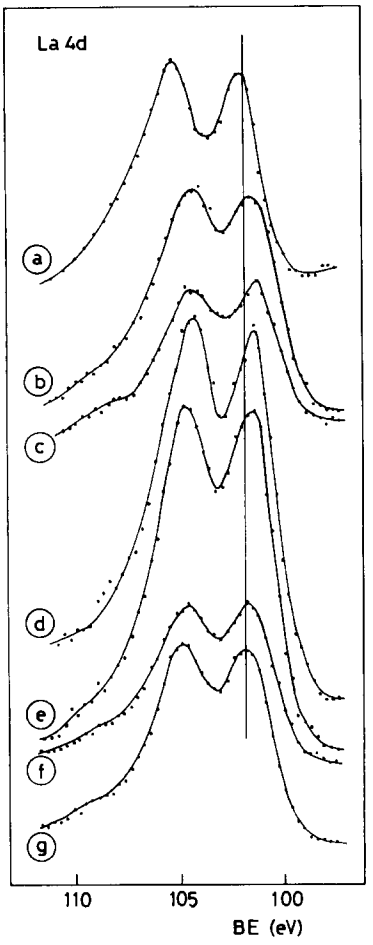

FIG. 5. La4*d* core level spectra of $LaTi_{0.6}Cu_{0.4}O_3$ sample. Notation is the same as in Fig. 4.

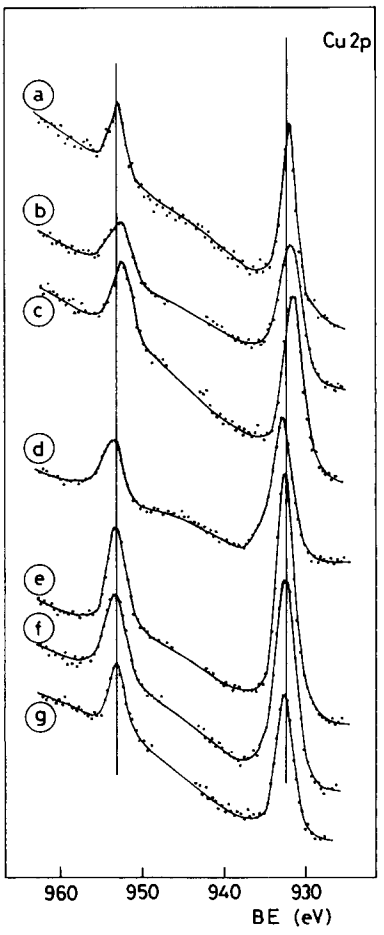

FIG. 6. Cu2*p* core level spectra of $LaTi_{0.6}Cu_{0.4}O_3$ sample. Notation is the same as in Fig. 4.

the high BE side: the BE of the maxima are typical of lattice O^{2-} ions, while the tail at higher BE is assigned to less electron-rich oxygen species, such as OH^- (*5, 13, 28–33*). The presence of other O-species with a net charge of one, such as O^- or O^{2-} is extremely unlikely, given their high reactivity. These results are consistent with the formation of a LaO(OH) compound by reaction of surface La_2O_3 with water produced in the reduction. The presence of LaO(OH) in H_2-reduced samples is supported by the appearance of a tail in the high BE side of the La4$d_{3/2}$ peak (Fig. 5), due to overlapping of

TABLE II

BINDING ENERGIES (eV) OF CORE ELECTRONS IN $LaTi_{0.6}Cu_{0.4}O_3$ PEROVSKITES SUBJECTED TO SEVERAL PRETREATMENTS

Pretreatment	O 1*s*	Ti $2p_{3/2}$	Cu $2p_{3/2}$	La $4d_{5/2}$
Vacuum, 723 K	529.8	458.3	931.8	102.1
H_2, 473 K	529.2	457.6	931.9	101.5
H_2, 523 K	529.0	458.0	931.6	100.9
H_2, 573 K	529.4	457.9	932.7	101.5
H_2, 623 K	528.9	458.4	932.4	101.0
H_2, 673 K	529.4	457.8	932.7	101.4
H_2, 723 K	529.9	457.9	932.0	101.9

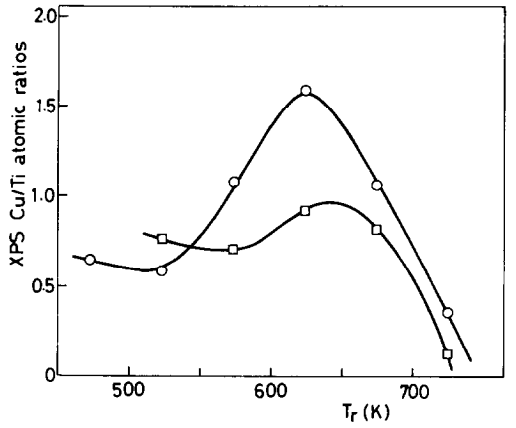

FIG. 7. Changes of the XPS Cu/Ti atomic ratios undergone by $LaTi_{1-x}Cu_xO_3$ samples when subjected to H_2-reduction treatments. □, $x = 0.2$; ○, $x = 0.4$.

a less intense La4*d* doublet with the more intense one of the La_2O_3 phase, the former assigned to lanthanum oxyhydroxide (*13*).

The BE's of Cu2*p* electrons found after different pretreatments are very similar (Fig. 6, Table II). These values in the range 931.6–932.7 eV are substantially lower (ca. 1.2 eV) than that of Cu^{2+} ions. In addition, no satellite peaks in the high BE side of the principal Cu2*p* peak, characteristic of Cu^{2+} species (*33*), have been detected. All these facts led to the conclusion that both outgassing and reduction pretreatments give rise to reduced copper species, very probably Cu° since the perovskite surface proves to be much easier to reduce than the bulk.

To get an idea of the changes undergone by copper upon H_2-reduction, the Cu/Ti atomic ratios have been calculated. In this calculation, normalized intensities for the number of scans and published sensitivity factors (*34*) have been considered. In Fig. 7 the XPS Cu/Ti atomic ratios of La $Ti_{0.8}Cu_{0.2}O_3$ and $LaTi_{0.6}Cu_{0.4}O_3$ samples are plotted against the reduction temperature. It is observed that the Cu/Ti ratio of the $LaTi_{0.6}Cu_{0.4}O_3$ sample reduced at $T_R \leq 523$ K almost coincides with the theoretical one (Cu/Ti = 0.67) for the stoichiometric perovskite, while in the same temperature range this ratio is ca. three times higher than the nominal composition (Cu/Ti = 0.25) in the $LaTi_{0.8}Cu_{0.2}O3$ sample. In agreement with XRD data (Fig. 1), this indicates that for substitution $x = 0.2$, Cu^{2+} ions are presumably incorporated to a separate phase different from perovskite. Furthermore, the XPS Cu/Ti ratios increase in both samples at higher reduction temperatures, and they reach a peak ca. 623 K with a subsequent decrease at higher temperatures. These results show that copper diffuses toward the surface upon reduction, attaining maximum exposure at temperatures close to 623 K while important sintering of copper particles takes place at higher temperatures. This finding emphasizes the importance of perovskite reduction and it determines the optimum temperature window to obtain maximum copper exposure as required in catalytic studies.

Conclusion

Compounds of the type $LaTi_{1-x}Cu_xO_3$ have been shown to have the perovskite structure only in the composition range $0.3 \leq x \leq 0.8$. For the unsubstituted ($x = 0$) and partially substituted ($x = 0.2$) compounds, the only phases present were $La_2O_3 \cdot 2TiO_2$ and $La_2O_3 \cdot 3TiO_{1.9}$ in the former case, and these two mixed oxides and CuO, La_2CuO_4, and $2La_2O_3 \cdot 3TiO_2$ in the latter. For the fully substituted ($x = 1.0$) compound, only CuO and La_2CuO_4 phases were detected. Although the synthesis of $LaCuO_3$ has been reported (*15*), this perovskite is not stable under the experimental conditions used in this work.

Copper-containing samples with substitutions $0.2 \leq x \leq 0.8$ revealed two reduction steps of Cu^{2+} to Cu°. The first, taking place at a low temperature and in a very narrow temperature window, is due to the separate CuO phases, and the second one at higher

temperatures and extending over a very large temperature range is due to the perovskite phase. This latter finding clearly illustrates the increased stability of copper ions in the perovskite structure. Finally, as revealed by XPS data, the most favorable conditions for obtaining a highly dispersed copper phase on the $La_2O_3 \cdot xTiO_2$ matrix were found to be those attained by H_2-reduction of $LaTi_{0.6}Cu_{0.4}O_3$ perovskite at temperatures very close to 623 K.

Acknowledgment

This work has been sponsored by the Comision Interministerial de Ciencia y Tecnología, Spain, under Project MAT 88/0161.

References

1. F. S. Galasso, "Structure, Properties and Preparation of Perovskite-Type Compounds," Pergamon, Oxford, 1969.
2. J. B. Goodenough and J. M. Longo, in "Landolt-Börnstein New Series" (K. H. Hellwege and A. M. Hellwege, Eds.), Vol. 4, part A, p. 126, Springer Verlag, Berlin, 1970.
3. J. B. Goodenough, *in* "Solid State Chemistry" (C. N. R. Rao, Ed.), p. 215, Dekker, New York, 1974.
4. S. Nomura, in "Landalt-Bornstein New Series" (K. H. Hellwege and A. M. Hellwege, Eds.), Vol. 12, part A, p. 368, Springer Verlag, Berlin, 1978.
5. L. G. Tejuca, J. L. G. Fierro, and J. M. D. Tascon, *Adv. Catal.* **36,** 237 (1989).
6. R. J. H. Voorhoeve, D. W. Johnson, Jr., J. P. Remeika, and P. K. Gallagher, *Science* **195,** 827 (1977).
7. P. R. Watson and G. A. Somorjai, *J. Catal.* **74,** 282 (1982).
8. G. A. Somorjai and S. M. Davis, *CHEMTECH* **13,** 502 (1983).
9. H. J. Gysling, J. R. Monnier, and G. Apai, *J. Catal.* **103,** 407 (1987).
10. J. R. Monnier and G. Apai, Prepr., *Div. Pet. Chem. Amer. Chem. Soc.* **31**(2), 239 (1986).
11. J. A. Broussard and L. E. Wade, Prepr., *Amer. Chem. Soc. Pap. Div. Fuel Chem.* **31**(3), 75 (1986).
12. J. A. Brown-Bourzutschky, N. Homs, and A. T. Bell, *J. Catal.* **124,** 41 (1990).
13. M. L. Rojas, J. L. G. Fierro, L. G. Tejuca and A. T. Bell, *J. Catal.* **124,** 52 (1990).
14. J. M. D. Tascón, S. Mendioroz, and L. G. Tejuca, *Z. Phys. Chem. Neue Folge* **124,** 109 (1981).
15. G. Demazeau, C. Parent, M. Ponchard, and P. Hagenmuller, *Mater. Res. Bull.* **7,** 913 (1972).
16. P. K. Gallagher, D. W. Johnson, Jr., and E. M. Vogel, *J. Amer. Ceram. Soc.* **60,** 28 (1977).
17. E. M. Vogel, D. W. Johnson, Jr., and P. K. Gallagher, *J. Amer. Ceram. Soc.* **60,** 31 (1977).
18. V. M. Goldschmidt, *Skr. Nor. Vidensk. Akad., Kl. 1: Mat. Naturvidensk, Kl.* No. 8 (1926).
19. M. Crespin, P. Levitz, and L. Gatineau, *J. Chem. Soc. Faraday Trans.* **2,** 79, 1181 (1983).
20. T. Nakamura, G. Petzow, and L. J. Gauckler, *Mater. Res. Bull.* **14,** 649 (1979).
21. J. L. G. Fierro, J. M. D. Tascón, and L. G. Tejuca, *J. Catal.* **93,** 83 (1985).
22. H. Van Damme and W. K. Hall, *J. Catal.* **69,** 371 (1981).
23. M. Avudaithai and T. R. N. Kutty, *Mater. Res. Bull.* **22,** 641 (1987).
24. Q. S. Li, K. Domen, S. Naitio, T. Onishi, and K. Tamaru, *Chem. Lett.*, 321 (1983).
25. G. Nagasubramaniam, M. V. C. Sastri, and B. Viswanathan, *Indian J. Chem., Sect. A,* **16,** 242 (1978).
26. G. Nagasubramanian, B. Viswanathan, and M. V. C. Sastri, *Indian J. Chem., Sect. A,* **16,** 245 (1978).
27. Z. K. Jelinek, "Particle Size Analysis," Chapter 2, Ellis Horwood, New York, 1974.
28. L. G. Tejuca, A. T. Bell, J. L. G. Fierro, and M. A. Peña, *Appl. Surf. Sci.* **31,** 301 (1988).
29. L. G. Tejuca and J. L. G. Fierro, *Thermochim. Acta* **147,** 361 (1989).
30. N. Yamazoe, Y. Teraoka, and T. Seiyama, *Chem. Lett.* 1767 (1981).
31. S. J. Cochran and F. P. Larkius, *J. Chem. Soc., Faraday Trans. I* 81, 2179 (1985).
32. J. A. Marcos, R. H. Buitrago, and E. A. Lombardo, *J. Catal.* **105,** 95 (1987).
33. P. Salvador, J. L. G. Fierro, J. Amador, C. Cascales, and I. Rasines, *J. Solid State Chem.* **81,** 240 (1989).
34. C. D. Wagner, L. E. Davis, M. V. Zeller, J. A. Taylor, L. H. Raymond, and L. H. Gale, *Surf. Interface Anal.* **3,** 211 (1981).